Available online at www.sciencedirect.com
ScienceDirect
Journal of Molecular Catalysis A: Chemical 264 (2007) 220–226
JOURNAL OF MOLECULAR CATALYSIS A: CHEMICAL
www.elsevier.com/locate/molcata

Experimental and semiempirical studies of effect of MCM-41 and cation exchanged zeolite Y on rate enhancement and diastereoselectivity of Diels–Alder reaction of *p*-benzoquinone and some derivatives with cyclopentadiene

Gholamreza Mashayekhi [a], Mehdi Ghandi [a,*], Faezeh Farzaneh [b], Mansour Shahidzadeh [a], Heydar Mahmoudi Najafi [c]

[a] *School of Chemistry, University College of Science, University of Tehran, Tehran, Iran*
[b] *Department of Chemistry, University of Alzahra, Tehran, Iran*
[c] *Iranian Research Organization for Science and Technology, Chemical Industries Research Center, Tehran, Iran*

Received 4 September 2006; received in revised form 16 September 2006; accepted 18 September 2006
Available online 23 September 2006

Abstract

The MCM-41 and zeolite Y exchanged with Li^+, Na^+, K^+ and Cs^+ were used as catalyst for Diels–Alder reaction of cyclopentadiene (CPD) with *p*-benzoquinone (PBQ) and some derivatives to achieve higher reaction rate and diastereoselectivity. The 2:1 CPD–PBQ adducts of *endo-anti-endo* and *endo-anti-exo* obtained, respectively, in the case of PBQ as the major product in the presencece of MCM-41 and CsY is remarkable. Semiempirical calculation by PM5 method was carried out to define the energetics of the system and Goering–Schewene diagram under the catalytic effect of BF_3 and $AlCl_3$ Lewis acids. It was found that even though the *endo-anti-exo* is thermodynamically more stable than *endo-anti-endo* in uncaytalyzed Diels–Alder reaction, the latter is the more stable isomer in the presence of Lewis acid catalyst.

Keywords: Diels–Alder; MCM-41; Zeolite Y; Heterogeneous catalyst

1. Introduction

The Diels–Alder (DA) reaction has been recognized as one of the most important methods for the construction of six-membered ring. Due to the concerted and orbital controlled reaction pathway, usually predictable stereoselectivity can be realized and making this reaction particularly useful in the stereoselective synthesis of various synthetic intermediates [1]. Although DA reactions are little influenced by polar factors, Lewis acids exert a strong catalyzing effect. Furthermore, Lewis acid catalyzed DA reactions are not only faster but also more stereoselective and more regioselective than the uncatalyzed reactions [1]. For this reason, the catalyzed reactions are of great importance. Many research have been done to improve the reaction rate and selectivity using homogenous Lewis acid [2,3], high pressure [4,5], and water as solvent [6]. Heterogenization of valuable homogeneous catalysts by either inclusion or immobilization within micropore or mesopore materials has several advantages such as reducing hazardous effluents and easier catalyst separation in harmony with sustainable green chemistry [7].

The cycloaddition reaction of cyclopentadiene (CPD) with *p*-benzoquinone (PBQ) is one of the oldest reactions named as DA reaction [8]. Theoretically, equimolar amount of PBQ, reacts easily with CPD to form a 1:1 cycloadduct [9], containing two isomers of *endo* as the major and *exo* as the minor product. The DA reaction with the 2:1 ratio of CPD to PBQ, on the other hand, affords the 1:1 cycloadduct and 2:1 adduct containing six stereoisomers as the major and minor products, respectively. With the exception of *exo-syn-exo* isomer, all the other five have been synthesized and characterized previously [10].

Mesoporous molecular sieves, which was synthesized by Mobile group in 1992 [11], have a space enough to accom-

* Corresponding author. Tel.: +98 21 88258977; fax: +98 21 66495291
E-mail address: ghandi@khayam.ut.ac.ir (M. Ghandi).

1381-1169/$ – see front matter © 2006 Published by Elsevier B.V.
doi:10.1016/j.molcata.2006.09.032

modate the guest molecules. The silicious MCM-41 exhibits a hexagonal array of one-dimensional mesoporous pore system ranging from 15 to 100 Å. Enlarging the pore size from micropore to mesopore region (>20 Å), and reducing the Lewis acid strength makes the MCM-41 to be different in comparison to zeolite [12]. The alminumsilicates known as the zeolites partly contain aluminum for silicon ions. This results in a network that bears a net negative charge. Compensation by other ions causes the zeolites to be positively charged within the channels, cavities and supercages [13]. Therefore, chemists have found this system as a brilliant host for the accommodated guest molecules in order to study either the positive field or the cavity confinement on reaction rate and product stereoselectivity.

In this investigation, we decided to investigate the DA reaction of PBQ, methylbenzoquinone, 2,5-dimethylbenzoquinone and 2,6-dimethylbenzoquinone with CPD in the presence of MCM-41 as solid acid catalyst. We also studied the same reactions under the effect of alkali metal exchanged zeolite Y in order to compare the catalytic activity of zeolite solid acid with those obtained with MCM-41. In order to minimize the surface reaction, we included the PBQ within the MCM-41 and zeolite pores by utilization of non-polar solvent. Therefore, no reaction was expected to occur prior to approaching the CPD molecules into the pores. Furthermore, to reduce the *ret*-DA possibility, all reactions were carried out at room temperature. To define the energenics of the system and Goering–Schewene diagram [14], semiempirical calculations was decided to be carried out by using PM5 method.

2. Experimental

2.1. Materials

PBQ and other derivatives were purchased from Aldrich and purified by sublimation before use. NaY zeolite was prepared and characterized according to the procedures described in the literature [15].

2.2. Preparation of cation exchanged zeolite Y

Monovalent cation (Li^+, K^+ and Cs^+) exchanged zeolites were prepared by stirring 10 g of NaY with 100 mL of 10% aqueous solution of the corresponding metal chloride for 12 h under reflux condition. The zeolites were filtered and washed thoroughly with distilled water for several times. This procedure was repeated for three times to ensure maximum exchange of cations of interest for Na^+ ions. The cation exchanged zeolites were then dried at 120 °C for 6 h. The exchanged percentages of Li^+, K^+ and Cs^+ were determined by atomic absorption spectroscopy as 73, 87 and 71, respectively.

2.3. Preparation of MCM-41

MCM-41 was synthesized and characterized according to the procedure previously described in literature by using hexadecyltrimethyl ammonium bromide as a template [16]. The product was calcined at 540 °C for 6 h to remove the template from the MCM-41 structure.

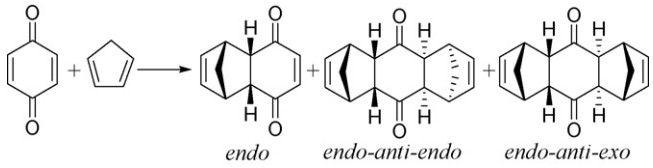

Fig. 1. Diels–Alder reaction of CPD with PBQ to *endo-anti-endo* and *endo-anti-exo* isomers.

2.4. Typical procedure for DA reaction

To a solution of 108 mg (1 mmol) of PBQ in 70 mL dry hexane, was added 2.0 g of activated MY zeolite or 4.0 g of MCM-41 (after pretreatment at 500 °C for 12 h), and the mixture was stirred under N_2 atmosphere at room temperature for 3 h. The slurry was filtered and washed with fresh hexane and then ether in order to remove the adsorbed PBQ on the zeolite surface. To the PBQ loaded zeolite in 70 mL hexane, was added 70 mg (or 145 mg) (1:1 or 2:1 mmol) of freshly distilled CPD in one portion and the slurry was stirred under N_2 atmosphere at room temperature for 3 h. The slurry was then filtered and washed with fresh hexane in order to remove any adsorbed unreacted CPD on zeolite surface. The product was extracted from zeolite cavities (or MCM-41) by stirring the solid in 80 mL of ether for 5 h. The slurry was filtered and the filtrate was evaporated by rotary evaporator. The residue was analyzed directly by using ^{1}H NMR to determine the diastereomeric ratio. The products were separated by column chromatography (ether–petroleum ether, 20:80), and characterized by comparison of their ^{1}H NMR with authentic samples.

2.5. Method of calculation

The structure of compounds was built by chemdraw, version 8 and was saved as MOPAC files by Chem3D for PM5 calculation. All calculations were done with WINMOPAC v.3.5.

3. Results and discussion

As seen in Table 1, in the absence of solid acid catalyst, equimolar amount of CPD with PBQ reacts to form 1:1 cycloadduct efficiently. Utilization of two equivalents of CPD under the similar condition produces only 13% of 2:1 adducts without catalyst (Fig. 1). Unfortunately, dimerization of CPD competes with this reaction because of the partial inactivation of 1:1 cycloadduct toward further DA reaction. The dicyclopentadine byproduct contaminates the main product(s) and cannot be separated easily. Consequently, the synthesis of 2:1 adduct in the absence of catalyst needs large excess amount of CPD to be complete [17]. On the other hand, a mixture of 90:10 *endo-anti-endo* to *endo-anti-exo* of 2:1 adduct stereoisomers in 94% yield is produced in the presence of mesoporous structure of MCM-41. Interstingly, this result is similar to that reported recently by Corma and co-workers [18]. We have included their results in

Table 1
Catalytic effect and diastereoselectivity of MY zeolite and MCM-41 on DA reaction of CPD with PBQ to 1:1 and 2:1 adducts

Catalyst	PBQ (mmol)	CPD (mmol)	Yield (%)	Selectivity (%)			
				1:1	2:1	*Endo-anti-endo*	*Endo-anti-exo*
–	1	1	87	100	–	–	–
LiY	1	1	89	33.8	66.2	62	38
CsY	1	1	80	34.0	66.0	43	57
–	1	2.1	74	87	13	76	24
LiY	1	2.1	88	2	98	57	43
NaY	1	2.1	82	5	95	50	50
KY	1	2.1	95	8	92	76	24
CsY	1	2.1	80	10	90	40	60
MCM-41	1	2.1	94	0	100	90	10
MCM-41[a]	1	3	90	0	100	91.4	8.6
Al–MCM-41[a]	1	3	94	0	100	65	35

[a] Results obtained at 60 °C are taken from Ref. [18].

Table 1 in order to make the comparison with our results more convenient. Based on their observation, the authors remarked that even though the *endo-anti-exo* is thermodynamically more stable, the kinetically controlled *endo-anti-endo* isomer has been produced as the major product [18]. Unfortunately, no explanation was provided for these speculations. Recall that the less stable 1:1 cycloadduct produced as the primary major product has the *endo* fusion in bicyclic product. This preference has arisen due to developing secondary interaction between the double bond LUMO present in five member ring and hexa-enedione HOMO present in six member ring at the transition state [19]. Since such secondary interaction is definitely absent in the second step toward the formation of the 2:1 adducts, the logic behind the mentioned kinetically preference for *endo-anti-endo* isomer cannot be envisaged easily. Moreover, they showed that the introduction of Al, Sn or Ti atoms in the framework enhances the DA reaction rate while preserving the selectivity to the *endo-anti-endo* isomer [18].

Suprisingly, the 2:1 adduct is obtained predominantly if the DA reaction is carried out within the zeolite cavities no matter to start with 1:1 or 2:1 ratio of CPD to PBQ. The major difference appears in reaction stereoselectivity with the latter ratio being the more selective toward the formation of 2:1 adduct. Diastereomeric ratio of 2:1 adduct depends on the cation type inside the zeolite supercages. Inspection of the results presented in Table 1 clearly indicates that with the exception of KY, increasing the cation size from Li^+, to Na^+ and then to Cs^+ directs the reaction to generate *endo-anti-exo* isomer in higher amount. In contrast to the DA reaction catalyzed by MCM-41 which afford the *endo-anti-endo* (90%) as the dominant isomer, the *endo-anti-exo* is obtained as the major product in the presence of CsY (60%). Based on the energy minimized structure obtained by MOPAC, the minimum sizes were determined as 8.58 and 8.38 Å for *endo-anti-endo* and *endo-anti-exo*, respectively. Therefore, the formation of the smaller stereoisomer as the major product within the zeolite Y exchanged with the largest Cs^+ cation with limitation in pore size is not surprising. On the contrary, under the kinetic conditions, obtaining the larger isomer, i.e., *endo-anti-endo* within the MCM-41 supercages with no limitation in pore size is anticipated. It is not possible to give a clear-cut explanation for K^+ irregularity. Some factors such as Coulomb interaction, the polarizability of the cation, and the average distance between the cations might be responsible for this observation [20].

In order to rationalize the results, the key role of benzoquinone complexed to the acid sites available within the MCM-41 or zeolite pores either in the primary step to the 1:1 CPD–PBQ adduct or in the second step affording the 2:1 adduct must be taken into consideration. Frontier molecular orbital (FMO) theory can successfully rationalize an enormous range of chemical phenomena. The significance of the highest occupied molecular orbital (HOMO) and lowest unoccupied molecular orbital (LUMO) become apparent since the interaction between non-degenerate orbitals is inversely proportional to the energy gap between the orbital. The smaller this gap, the interaction is stronger and reaction proceeds faster. The main orbital interaction in DA reaction is between the LUMO of dienophile and HOMO of the diene [1]. Electron withdrawing substituents on the dienophile double bond, and electron donating groups on diene accelerate the reaction by lowering the LUMO energy and raising the energy of HOMO orbital, respectively [1]. It is known that MCM-41 sample, owing to its short-range amorphous characteristics, strongly dealuminates during the activation procedure, leading to a sample with lower and weaker acidity [21]. The presence of weak Bronsted acid sites in MCM-41 was claimed to be responsible for the observed rate enhancement of DA reaction [18]. The LUMO energy of the 1:1 CPD–PBQ adduct either alone or complexed to BF_3 and $AlCl_3$ as the model of solid acid sites calculated by using the PM5 method is presented in Table 2. We have included the similar result for acrolein as a simple and well known dienophile in Table 2 in order to compare our results with those already present in literature. It is evident from Table 2 that the CPD–PBQ dienophile LUMO energy lowering due to complexation with BF_3 and $AlCl_3$ are 1.25 and 1.13 eV, respectively. As shown in Table 2, acrolein E_{LUMO} is lowered by 1.85 eV under the catalytic effect of BF_3. Recall that Houk and Munchausen [22] observed experimentally that tri-cyanoethylene was 10^6 times more reactive than acrylonitrile in DA reactions and had a LUMO energy that was lower by 2.06 eV. Aluminum chloride catalyzed DA reaction of

Table 2
LUMO energies and orbital coefficients of dienophile either alone or complexed to BF_3 and $AlCl_3$ Lewis acids

Structure	E_{LUMO} (eV)	Orbital coefficient		
		C1	C2	C3
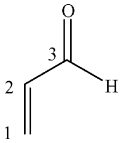	−0.53	−0.54	0.29	0.62
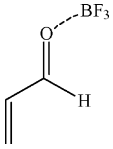	−2.38	0.52	−0.16	−0.70
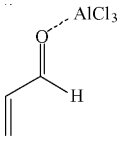	−2.06	0.51	−0.15	−0.70
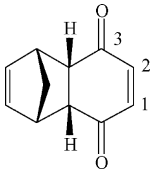	−1.24	0.36	0.36	0.36
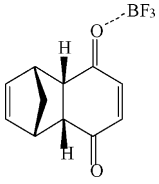	−2.49	−0.38	0.24	0.54
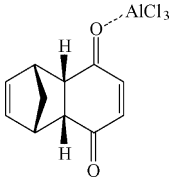	−2.37	+0.39	−0.26	−0.53

some dienes with methyl acrylate were experimentally shown to have the rate enhancement of 10^5 in comparison to uncatalyzed reaction [23–25]. Guner et al. [26] found a decrease in the LUMO energy of 2.63 eV for the acrolein–boron trifluoride complex based on ab initio calculations. Based on the latter result, the authors believed that the decrease of 2.63 eV for the acrolein–boron trifluoride complex is slightly larger than expected for the experimental rate increase of 10^5 to 10^6 times that have been reported for catalyzed reactions [26]. The decrease of 1.85 eV for acrolein–boron trifluoride complex obtained in our semiempirical calculations is closer to experimental results. Roughly speaking, it can be concluded that the rate enhancement due to 1.25 eV lowering of 1:1 CPD–PBQ LUMO energy is estimated about two to three numbers of magnitude. On the other hand, the energy difference in transition state stabilization calculated on the basis of the third term appears in Klopman's equation for DA reaction uncatalyzed and BF_3 catalyzed is shown in Table 3 [27]. Based on these results, and by knowing that the activation entropy for the catalyzed and uncatalyzed may be considered to be similar, the rate enhancement due to the presence of BF_3 catalyst is estimated about 10^2 to 10^3. This ratio is similar to that which was anticipated by E_{LUMU} lowering (*vide supra*).

Tables 4 and 5 present the calculated thermodynamic parameters for BF_3 catalyzed DA reaction of 1:1 CPD–PBQ adduct with CPD and *ret*-DA reactions of *endo-anti-endo* and *endo-anti-exo* at 25 and 60 °C, respectively. Comparison of the calculated ΔG_r°'s of uncatalyzed or thermal DA to *endo-anti-endo* and *endo-anti-exo* presented in Table 4 footnote with that for BF_3 catalyzed reaction clearly indicates that while the *endo-anti-exo* is more stable than the *endo-anti-endo* in uncatalyzed (thermal) DA reaction, the latter is the more stable isomer formed in the presence of BF_3 catalyst. Therefore, the formation of *endo-anti-endo* as the major product (90%) in catalyzed DA reaction is in agreement with the *Evans-Polanyi* principle (see Table 4) [28]. In other word, the more thermodynamically favored isomer is the more kinetically favored isomer as well. This result is not

Table 3
Stabilization energy of the DA transition state of BF_3 catalyzed with respect to uncatalyzed reaction

DA reactants		ΔE_1	ΔE_2	Total ΔE (eV)
		$\frac{2(c_{HOMO1}c_{LUMO1}\beta_{11})^2}{(E^{diene}_{HOMO} - E^{dienophile}_{LUMO})}$	$\frac{2(c_{HOMO4}c_{LUMO2}\beta_{24})^2}{(E^{diene}_{HOMO} - E^{dienophile}_{LUMO})}$	
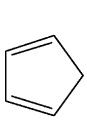	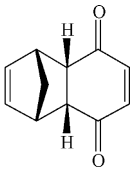	−0.40	−0.40	−0.80
	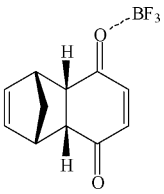	−0.53	−0.42	−0.95

Table 4
Thermodynamic parameters of BF_3 catalyzed DA reaction of 1:1 CPD–PBQ adduct with CPD at 25 and 60 °C

Reaction temperature, K (°C)	DA product	ΔH_r° (kcal/mol)	ΔS_r° (cal/K/mol)	ΔG_r° (kcal/mol)	$\Delta H^\#$ (kcal/mol)	$\Delta S^\#$ (cal/K/mol)	$\Delta G^\#$ (kcal/mol)
298 (25)	*Endo-anti-endo*	−29.00	−51.33	−13.71	7.66	−52.74	23.15
	Endo-anti-exo	−27.67	−50.77	−12.56	10.29	−50.20	25.19
333 (60)	*Endo-anti-endo*	−29.07	−51.52	−11.92	7.60	−52.96	24.58
	Endo-anti-exo	−27.64	−50.95	−7.99	10.24	−50.37	29.88

ΔG_r^0 for the formation of *endo-anti-endo* and *endo-anti-exo* in uncatalyzed (thermal) DA reactions were found by calculations as −11.14, −12.15 and −8.17, −9.59 kcal/mol at 25 and 60 °C, respectively.

Table 5
Thermodynamic parameters of BF_3 catalyzed *ret*-DA reaction of *endo-anti-endo* and *endo-anti-exo* adducts to1:1 CPD–PBQ adduct and CPD at 25 and 60 °C

Reaction temperature, K (°C)	*ret*-DA starting material	ΔH_r° (kcal/mol)	ΔS_r° (cal/K/mol)	ΔG_r° (kcal/mol)	$\Delta H^\#$ (kcal/mol)	$\Delta S^\#$ (cal/K/mol)	$\Delta G^\#$ (kcal/mol)
298 (25)	*Endo-anti-endo*	29.00	51.33	13.71	35.22	−1.97	35.51
	Endo-anti-exo	27.67	50.77	12.56	37.88	0.57	37.71
333 (60)	*Endo-anti-endo*	29.07	51.52	11.92	35.24	−2.00	35.83
	Endo-anti-exo	27.64	50.95	7.99	37.88	0.59	37.71

surprising since the BF_3 is complexed to the carbonyl group either in the 1:1 adduct starting material or in 2:1 adduct product. Moreover, such complexation not only stabilizes the transition state, but also stabilizes the product as well. This effect is consistent with Leffler assumption, which states that the *free energy of reaction will only be partially reflected in the free energy of activation* [29]. That the $\Delta\Delta G_r$ is smaller than $\Delta\Delta G^\#$ (see Fig. 2), may not be difficult to be interpreted since due to the breakage of the bonds in going from neutral reactants to neutral product, there are more partial charges present in the transition state than reactants and product [29].

Comparison of the distereoselectivitis obtained in DA reactions in the presence of Al–MCM-41 [18], and MY (M = alkaline cation), might reveals another aspect of these two solid acid catalysts. Recall that a mixture of 90:10 of *endo-anti-endo* to *endo-anti-exo* was obtained in the presence of Al–MCM-41 with the Si/Al molar ratio of 15 during 1 h at 60 °C [18]. On the other hand, a mixture of these two stereoisomers with less selectivities was formed when MY zeolite was used as catalyst (see Table 1). Such results may be interpreted easily since $\Delta\Delta G^\#$ is 5.30 and 2.04 kcal/mol, respectively (see Fig. 2 and Fig. 3). Moreover, as seen in Table 5, the $\Delta\Delta G_r^\circ$'s for BF_3 catalyzed DA reactions at 25 and 60 °C to *endo-anti-endo* and *endo-anti-exo* are 1.15 and 3.93 kcal/mol, respectively. This means that the reaction is more selective at 60 °C under kinetic conditions (lower time). The selectivity in the case of Al–MCM-41 decreased to 65:35 when the reaction was prolonged to 6 h (thermodynamic condition) [18]. This effect was explained by the occurrence of *ret*-DA

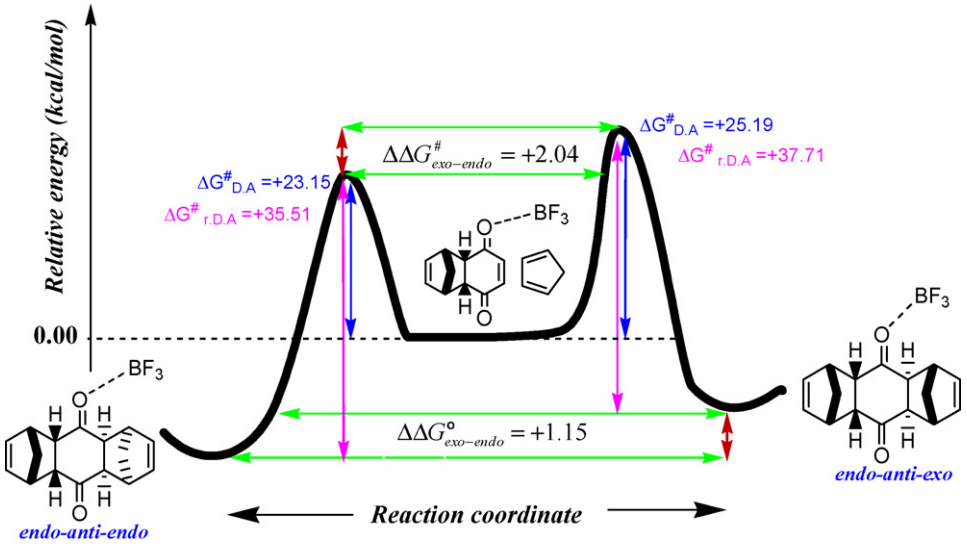

Fig. 2. The Goering–Schewene diagram of BF_3 catalyzed DA reaction to *endo-anti-endo* and *endo-anti-exo* isomers and BF_3 catalyzed *ret*-DA reactions of *endo-anti-endo* and *endo-anti-exo* to 1:1 of CPD–BQ adduct and CPD at 25 °C.

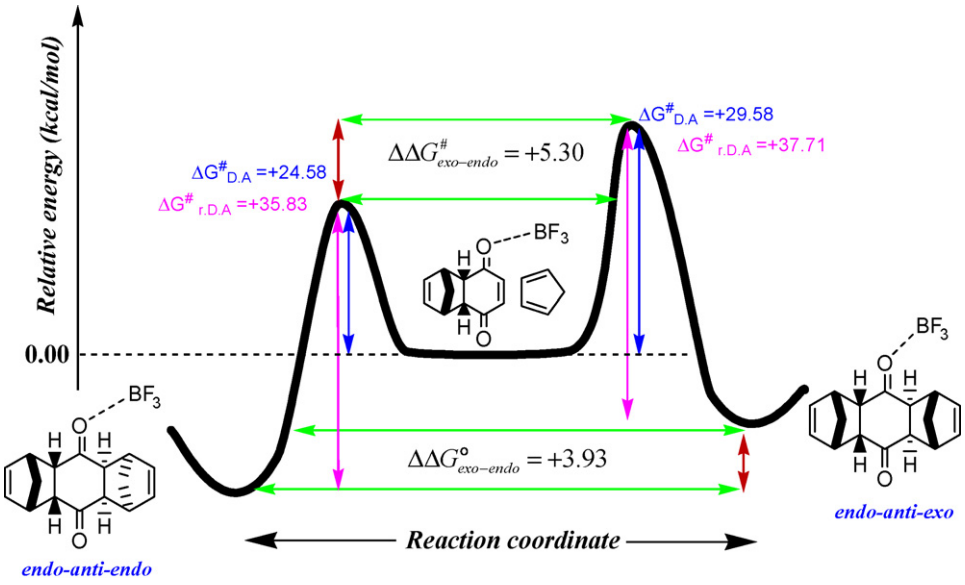

Fig. 3. The Goering–Schewene diagram of BF_3 catalyzed DA reaction to *endo-anti-endo* and *endo-anti-exo* isomers and BF_3 catalyzed *ret*-DA reactions of *endo-anti-endo* and *endo-anti-exo* to1:1 CPD–PBQ adduct and CPD at 60 °C.

reaction promoted by the higher bronsted acid sites present in Al–MCM-41 [18]. In contrary, the incorporation of Al within the MCM-41 network has interpreted to increases the number of Lewis acid sites based on the pyridine adsorption experiments [30]. The dispute has yet to be resolved. To make insight into the energetic of system, the Goering–Schewene diagrams [14] for the BF_3 catalyzed DA reactions at 25 and 60 °C are shown in Figs. 2 and 3. As seen in Fig. 3, under the thermodynamic conditions (60 °C and 6 h), it is the *endo-anti-endo* isomer, which must be accumulated as the major product. Obtaining the 65:35 of the *endo-anti-endo* to *endo-anti-exo* isomer in the presence of Al–MCM-41 during 6 h at 60 °C [18], is consistent with the energy diagram. The authors believed that the change in the ratio was promoted by the occurrence of *ret*-DA reaction during 6 h. Due to the presence of many acid sites either Bronsted or Lewis in Al–MCM-41 (similar to homogeneous BF_3 or $AlCl_3$), the occurrence of the *ret*-DA with the free energies of activation of 35.83 and 37.71 kcal/mol, respectively, for *endo-anti-endo* and *endo-anti-exo* (see Table 5 and Fig. 3) at 60 °C is anticipated. Recall that the *ret*-DA in our experiments is not likely to happen at room temperature (25 °C) due to the high free energies of activation in the absence of efficient thermal energy (35.51 and 37.71 kcal/mol, see Table 4 and Fig. 2). Therefore, it can be concluded that the formation of both stereoisomers within MY zeolite has arisen from DA condensation of CPD–PBQ with CPD. For this, the MY zeolite should be more acidic than Al–MCM-41 with the molar ratio of Si/Al = 15 (*vide supra*).

In the next step, the reaction of a number of PBQ derivatives such as methyl-benzoquinone, 2,5-dimethylbenzoquinone and 2,6-dimethylbenzoquinone with CPD were investigated in the presence of MY zeolites and MCM-41 (Fig. 4). We have not specified the cation type in MY since no differences were observed in their reactivities. The results are presented in Table 6. In contrast to PBQ, the 1:1 cycloadducts are produced as the main products by using the PBQ derivatives. As seen in Table 6,

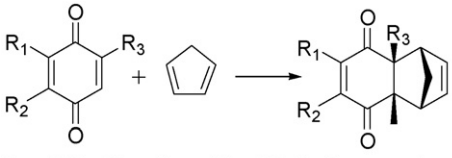

$R_1 = CH_3$, $R_2 = R_3 = H$: Methylbenzoquinone
$R_1 = H$, $R_2 = R_3 = CH_3$: 2,5-Dimethylbenzoquinone
$R_2 = H$, $R_1 = R_3 = CH_3$: 2,6-Dimethylbenzoquinone

Fig. 4. Diels–Alder reaction of CPD with PBQ to 1:1 cycloadducts.

the higher product yields are generated in the presence of either cation exchanged zeolites Y or MCM-41. Moreover, products with more purity are obtained under these conditions. That the 2:1 adducts similar to PBQ are not obtained in these cases were anticipated since the 2:1 adduct of methylbenzoquinone with CPD has been produced either under high pressure [5], or by using 5 M lithium percholrate in ether [31]. It is worth noting that the dipolemoment changes from 1:1 to 2:1 adduct was calculated as 2.86 to 4.15 Debyes, respectively. Therefore, the formation of 2:1 adduct in the case of methylbenzoquinone in

Table 6
Catalytic effect of MY and MCM-41 on DA reaction of CPD with some PBQ derivatives

Dieneophile	Catalyst	Time (h)	Yield (%)
Methylbenzoquinone	–	5	60
	MY	3	90
	MCM-41	3	96
2,5-Dimethylbenzoquinone	–	5	50
	MY	3	85
	MCM-41	3	95
2,6-Dimethylbenzoquinone	–	5	45
	MY	3	75
	MCM-41	3	84

the presence of 5 M lithium percholrate in ether is rationalized. The formation of 2:1 adducts of 2,5-dimethylbenzoquinone and 2,6-dimethylbenzoquinone with cyclopentadiene have not been reported so far. Recall that on the basis of PM5 calculations, the free energy of activation for 2:1 adduct of CPD to 2,6-dimethylbenzoquinone at 25 and 60 °C were found as 46.37 and 48.18 kcal/mol, respectively.

4. Conclusion

In summary, our study reveals that zeolite Y and MCM-41 enhance the DA reaction rate of PBQ and the corresponding monomethyl and dimethyl derivatives with CPD. We have also exhibited the influence of the MCM-41 and cation present within the zeolite Y cavities on reaction diastereoselectivity. Moreover, it was shown that the semiempirical calculatios are useful in understanding the kinetic and thermodynamic of systems used in this research.

Acknowledgement

The authors would acknowledge the Research Council of the University of Tehran for financial support of this research.

References

[1] I. Fleming, Frontier Orbitals and Organic Chemical Reactions, John Wiley and Sons, 1976, pp. 106–148.
[2] S. Yamabe, T. Dai, T. Minato, J. Am. Chem. Soc. 117 (1995) 10994.
[3] J. Howarth, K. Hanlon, D. Fayne, P. McCormac, Tetrahedron Lett. 38 (1997) 3097.
[4] G. Issaacs, Chem. Ber. (1987) 47.
[5] S. Srivastava, A.P. Marchand, V. Vidyasagar, J.F. Flippen-Anderson, R. Gilardi, C. George, Z. Zachwieja, W.J. le Noble, J. Org. Chem. 54 (1989) 247.
[6] C.J. Li, Chem. Rev. 105 (2005) 3095.
[7] R.I. Kureshy, I. Ahmad, N.H. Khan, S.H.R. Abdi, K. Pathak, R.V. Jasra, J. Catal. 238 (2006) 134.
[8] O. Diels, K. Alder, Ann. Chem. 98 (1928) 460.
[9] A.P. Marchand, R.W. Allen, J. Org. Chem. 39 (1974) 1596.
[10] P. Yates, K. Switlak, Can. J. Chem. 68 (1990) 1894.
[11] J.S. Beck, J.C. Vartuli, W.J. Roth, M.E. Leonowicz, C.T. Kresge, K.D. Schmitt, C.T. Chu, D.H. Olson, E.W. Sheppard, S.B. McCullen, J.B. Higgins, J.L. Schlenker, J. Am. Chem. Soc. 114 (1992) 10834.
[12] K. Shanmugapriya, M. Palanichamy, V.V. Balasubramanian, V. Murugesan, Micropor. Mesopor. Mater. (2006) 273.
[13] R. Szcostak, Molecular Sieves Principles of Synthesis and Identification, Van Nostrand Reinhold, New York, 1989.
[14] H.L. Goering, C.B. Schewene, J. Am. Chem. Soc. 87 (1965) 3516.
[15] F. Farzaneh, J. Soleimannejad, M. Ghandi, J. Mol. Catal. A 118 (1997) 223.
[16] Q. Cai, W.Y. Lin, F.S. Xiao, W.Q. Pang, J. Micropor. Mesopor. Mater. 32 (1999) 1.
[17] R. Brown, J.M. Bruce, D.W. Hudson, O.S. Mills, J. Chem. Soc., Perkin Trans. 2 (1974) 132.
[18] M. Victoria Gomez, A. Cantin, A. Corma, A. de la Hoz, J. Mol. Catal. A 240 (2005) 16.
[19] T.H. Lowry, K.S. Richardson, Mechanism and Theory in Organic Chemistry, Happer Collins, New York, 1987, pp. 925–926.
[20] I. Hannus, I. Kiricsi, P. Lentz, J.B. Nagy, Colloid Surf. A-Physicochem. Eng. Asp. 158 (1999) 29.
[21] I. Rodringuez, M.J. Climents, S. Ibbora, V. Fornes, A. Corma, J. Catal. 192 (2000) 441.
[22] T.N. Houk, L.L. Munchausen, J. Am. Chem. Soc. 98 (1976) 937.
[23] T. Inukai, T. Kojima, J. Org. Chem. 32 (1967) 872.
[24] T. Inukai, T. Kojima, J. Org. Chem. 31 (1966) 1121.
[25] T. Inukai, T. Kojima, J. Org. Chem. 36 (1971) 924.
[26] O.F. Guner, R.M. Ottenbrite, D.D. Shillady, V. Alstron, J. Org. Chem. 52 (1987) 391.
[27] G. Klopman, Chemical Reactivity and Reaction Paths, John Wiley & Sons, New York, 1974, pp. 55–67.
[28] M.J.S. Dewar, R.C. Dougherty, The PMO Theory of Organic Chemistry, Plenum, New York, 1975, pp. 210–220.
[29] A. Pross, Theoretical and Physical Principles of Organic Reactivity, John Wiley & Sons, New York, 1995, pp. 177–180.
[30] A. Satasuma, Y. Segawa, H. Yoshida, T. Hattori, Appl. Catal. A Gen. 264 (2004) 229.
[31] P.A. Grieco, J.J. Nunes, M.D. Gaul, J. Am. Chem. Soc. 112 (1990) 4595.